Numerical analysis and statistical description of the primary breakup in fuel nozzles of large two stroke engines for the application in CFD engine simulations

*Sebastian Hensel, Kai Herrmann, Reiner Schulz and German Weisser

Wärtsilä Switzerland Ltd, PO Box 414, Zürcherstr. 12, CH-8401 Winterthur, Switzerland

Key Words: Large two stroke engines, CFD, Spray, Fuel Injection, Nozzle, LES

ABSTRACT

In this work, the in-nozzle flow and primary breakup of fuel nozzles applied in large two stroke engines was analyzed by combined RANS and LES simulations. Intensive investigations have been performed to describe the influence of geometrical design features and flow conditions inside the nozzle on the droplet diameters, velocities and locations of origin. It is shown that the spray and droplet formation in large two stroke engines is highly unsymmetrical and depends on the nozzle geometry, location of the orifice and also on the upstream flow conditions. Disturbances and a sharp redirection of the flow into the nozzle orifice lead to a deflection of the dense fuel core, while an eccentricity of the nozzle bore induces a wrinkling up and rotation of the dense core around its central axis. Both phenomena lead to an asymmetrical disintegration of the liquid core.

To describe the primary breakup and the aforementioned phenomena in CFD in-cylinder simulations, prior in-nozzle flow or LES simulations are realistically not manageable and inefficient, as they require extensive computational effort. Hence, a statistical model to describe the primary breakup in Lagrangian spray simulations is introduced. Depending on thermodynamic conditions and nozzle geometry, droplet parcels are generated around the dense core by using probability density functions (PDF) for the droplet diameter, velocity and location. The PDFs as well as correlations for the dense core length, deflection of the spray and mean droplet diameter were derived from LES simulations.

INTRODUCTION

To describe the primary breakup, numerous models exist that were mainly generated for the application in automotive or heavy duty engines development. These models are divided into several classes due to the driving mechanisms they are based on, as cavitation [1][2][3], aerodynamics [4] or turbulence [5]. The models differ in complexity and amount of data required for the calculation of the spray. Simple models are based on assumptions for the conditions inside the nozzle leading to uncertainties and a loss in quality [6]. Otherwise, several complex models require prior CFD simulations of the in-nozzle flow, resulting in high computational effort and inefficiently long development cycles.

The application of models developed for automotive size engines to simulations of marine diesel engines often gives quite promising results. However, the parameters affecting the spray dynamics in marine diesel engines differ substantially from automotive type engines, due to both, fuel properties and size [7]. Based on the geometric arrangement of the orifice and the upstream conditions the spray core decays asymmetrically, rotates and is deflected. Most of the existing models do not describe these processes or combinations of these and they are not validated for nozzle diameters and fuel mass flows of large 2S marine diesel engines. Furthermore, in these engines, mechanisms as cavitation inside the nozzle only have minor influence on the droplet formation. Hence, most of the existing models are not practical or require intensive adaption to ensure an accurate description of the primary breakup.

The in-nozzle flow and primary breakup of fuel nozzles applied in large two stroke engines was analyzed numerically and experimentally in this work. A first approach was generated to describe the primary breakup statistically based on thermo- and fluid dynamic conditions and geometric boundaries. The first results of the model are satisfying. Despite this, further extension and upgrading of the model as well as further validation by new experimental data (PDA-measurements) is planned in the next project phase (HERCULES-C).

EXPERIMENTAL SETUP

For validation, shadow images obtained in a spray and combustion chamber (SCC) under different conditions were used. This optical accessible constant volume chamber has a diameter of 500 mm and allows the non-intrusive investigation of in-cylinder processes such as fuel injection and evaporation, ignition, combustion and emission formation under realistic conditions. A detailed description of the SCC is given in [8]. Fig. 1 shows the SCC setup and Fig. 2 shows shadow images of the spray for different time steps. Due to the swirl, the spray breaks up asymmetrically and is bent.

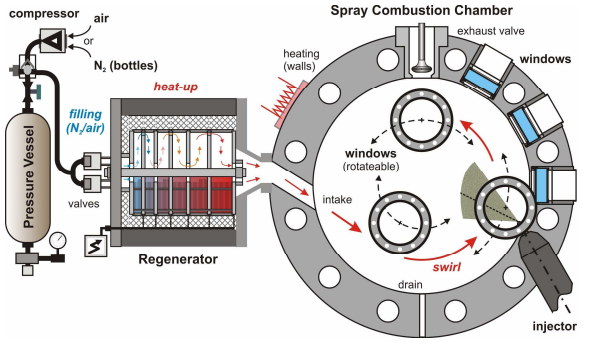

Fig. 1: Spray and Combustion Chamber (SCC)

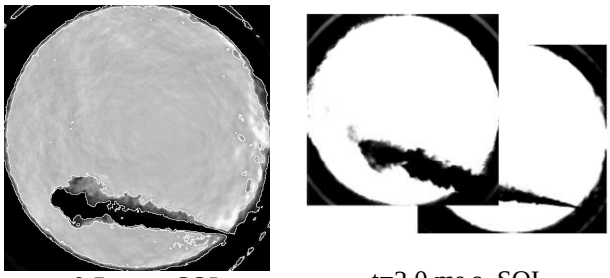

t=0.5 ms a. SOI t=2.0 ms a. SOI

Fig. 2: Shadow images of the spray, p=90 bar, T=900 K, swirl

IN-NOZZLE FLOW SIMULATIONS (RANS)

To generate the boundary and initial conditions for LES simulations of the primary breakup, transient RANS simulations (VOF method) of the in-nozzle flow were carried out beforehand. Therefore the atomizer nozzle, the needle and part of the supply system were modeled (see Fig. 3). The needle movement and the transient pressure profiles at the boundaries were derived from experimental data.

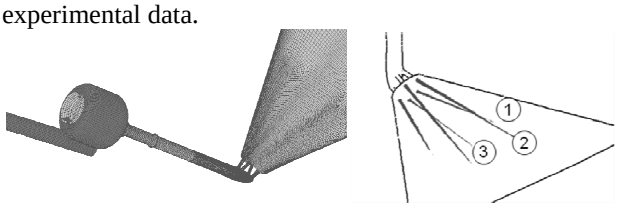

Fig. 3: Model of the injector atomizer, including needle seat and supply system

PRIMARY BREAKUP SIMULATIONS (LES)

LES simulations of different atomizer nozzles were performed. Therefore the flow inside a single nozzle bore and in the connected downstream plenum volume (length about 30-50mm) was simulated on the basis of the VOF method (compare Fig. 4). The cell size in the centre and in regions of the primary breakup is about 15µm, resulting in meshes with 5 to 8 million cells. The time step size was adapted to a maximum Courant number of 1, resulting in average Courant numbers about 0.02. The boundary conditions and the initial conditions are imported from transient RANS simulations.

The results of the primary breakup simulation show that the spray and droplet formation in large two stroke engines is highly unsymmetrical and depends on the nozzle geometry, location of the orifice and also on the upstream flow conditions. Disturbances and a sharp redirection of the flow into the nozzle orifice lead to a deflection of the dense fuel core, while an eccentricity of the nozzle bore induces a wrinkling up and rotation of the dense core around its central axis. Both phenomena lead to an asymmetrical disintegration of the liquid core, shown in Fig. 5.

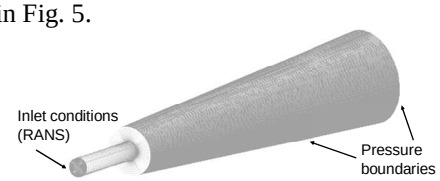

Fig. 4: Model for LES simulations of the flow inside a single nozzle bore and the connected downstream plenum

Fig. 5: Visualization of the interfaces between gas and spray (VOF=0.01) and spray and liquid (VOF=0.99); Eccentric located orifice leading to a wrinkling up and rotation of the core

The primary breakup of the bores 1, 2 and 3 of a standard injector (compare Fig. 3) was analyzed, regarding the effects of the bore position and geometric arrangement on the shape and decay of the dense core (Fig. 5). The aforementioned processes could clearly be identified. A sharp redirection of the flow into the nozzle orifice leads to a deflection of the dense fuel core and an asymmetric spray breakup. An eccentricity of the nozzle bore induces a wrinkling up and rotation of the dense core around its central axis. A sharp redirection of the flow into an eccentric bore leads to a superposition of both effects.

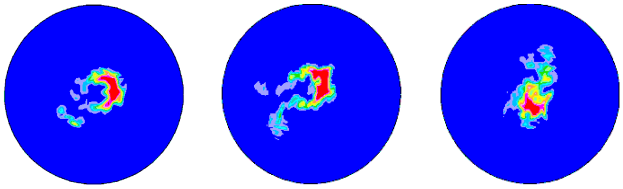

Bore 1 Bore 2 Bore 3

Fig. 6: Cross sections through liquid core perpendicular to the orifice axis at a distance of 15 times the nozzle diameter. Bore 1 & 2: Eccentric orifice. Bore 3: Symmetrically placed orifice.

However, the primary breakup is also influenced by the flow inside the atomizer. The narrow arrangement of the bores leads to interfering flow phenomena and additional disturbances. Hence, a quantitative analysis of separate effects is hardly possible by analyzing the flow and primary breakup of a standard atomizer with several bores. Furthermore it is not possible to identify separate sprays in the SCC for model validation. Hence, the influence of different vertical flow angles on the primary breakup, spray deflection and asymmetry of the spray formation was brought into focus. Therefore, atomizers with just one symmetrically placed bore were investigated numerically and experimentally. Thus, a

rotation of the spray is not expected. The vertical angle was varied in steps of 10°. Furthermore, the bore diameter to length ratio was varied for the atomizer with a vertical nozzle angle of 10°. The nozzle specifications are given in Table 1.

Nozzle No. [-]	1	2	3	4	5	6
Vert. angle [°]	0	10	20	30	10	10
Diam. [mm]	0.95	0.95	0.95	0.95	1.05	0.85
Length [mm]	4	4	4	4	4	4

Table 1: Atomizer configurations

For illustration, Fig. 7 shows cross sections of the atomizers 1, 2 and 3 with vertical nozzle angles of 0°, 10° and 20°.

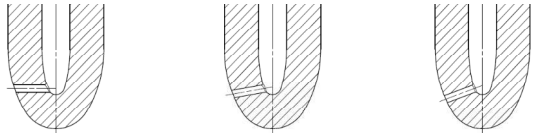

Nozzle 1 (0°) Nozzle 2 (10°) Nozzle 3 (20°)

Fig. 7: Atomizers with different vertical nozzle angles

The fuel properties and injection conditions are given in the following table:

Diesel surrogate (simulation)	C12H26
density ρ	750 kg/m^3
Viscosity μ	0.00137 kg/ms
Surface tension σ	0.024868 N/m
Fuel rail pressure p_f	700 bar
Backpressure p_g	90 bar
Injection duration TI	14 CAD @ 100 rpm

Table 2: Fuel properties and injection conditions

Fig. 8 shows exemplarily the liquid core and the primary breakup of the nozzles with 10° and 20° vertical angle. The dense liquid core is characterized by cells with VOF>0.99 that are still connected to the nozzle. In both cases the spray formation is highly asymmetric, with a dense core on the lower and resolved droplets breaking away on the upper side. With 10° the penetration length of the dense core is smaller than with 20°.

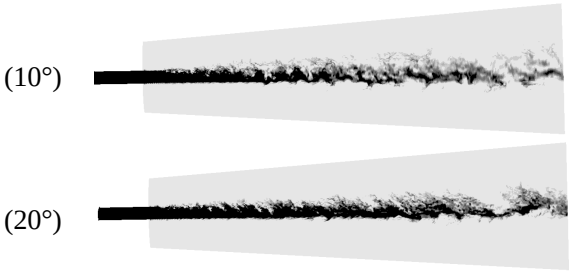

Fig. 8: Dense core and primary breakup of nozzles with 10° and 20° vertical angle

Furthermore it can be observed that the dense core is breaking up due to Kevin Helmholtz instabilities growing on the surface of the dense core. The turbulence generated inside the nozzle bore induces surface waves on the whole surface of the dense core. Pressure fluctuations as well as radial and axial velocity components are induced in both, the liquid core and the gas phase. Due to the high relative velocities between liquid and gas, resulting in high aerodynamic forces, these surface waves grow and induce the breakup of the dense core.

Fig. 9 shows the penetration length of the dense core calculated by LES simulations for different nozzle angles on top and for different bore sizes on the bottom. It is observed that the penetration length increases with decreasing redirection of the fluid flow. The penetration of the dense core does not change significantly, if the bore angle is varied from 0° to 10°. But with further increasing of the bore angle and less redirection of the flow, the penetration length increases exponentially. In contrast, the influence of the bore size on the penetration length of the dense core is in this range of bore diameters rather low. However, the penetration length increases slightly with bore diameter. For further investigation, simulations with smaller cross sections are planned to cover the whole range of bore diameters used in Wärtsilä's injector nozzles.

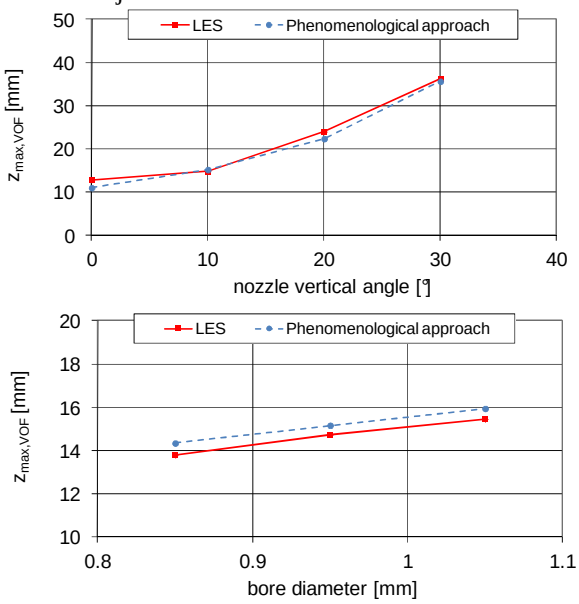

Fig. 9: Penetration length of the dense core depending on nozzle angle and bore size; Comparison between LES simulation and phenomenological approach

For the calculation of the location and droplet size in the statistical approach, estimations of either the mean or the maximum magnitudes are required. Phenomenological approaches were generated to estimate the breakup length of the dense core, the deflection of the spray and the maximum droplet diameter. To calculate the penetration length of the dense core, the approach of Hiroyasu [9] was modified and extended for the application on 2S-marine atomizers and deflected sprays:

$$L_{core} = 1.25 \cdot d \cdot \left(\frac{p_g}{\rho_f u_f^2}\right)^{0.05} \cdot \left(\frac{d}{l}\right)^{-0.5} \cdot \left(\frac{\rho_f}{\rho_g}\right)^{0.5} \cdot \frac{1}{(1-\sin\alpha)^{1.7}} \quad ; \quad 0° \le \alpha \le 40°$$

The values extracted from LES simulations and the results calculated by phenomenological approaches are also compared in Fig. 10 - Fig. 12.

In Fig. 10 the deflection angles of the dense spray core tip are shown for different nozzle angles, depending on time. Between each post file 1000 iterations were calculated, equivalent to about 1.5µs. The temporally averaged values are plotted as squares on the y-axis of the diagram. Due to the above mentioned surface waves the values are fluctuating. The fluctuations increase with the redirection of the flow as the turbulent breakup is intensified. For 0° vertical angle, it is not possible to identify the core tip angle due to the fast breakup and the quickly increasing wave amplitudes. Considering only the three cases 10°, 20° and 30°, an increasing deflection of the dense core with intensified redirection of the flow inside the nozzle is observed.

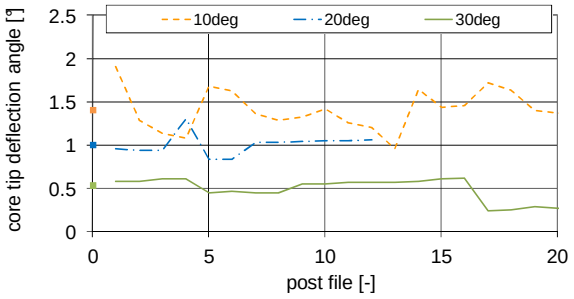

Fig. 10: Deflection angles of the dense spray core tip over time

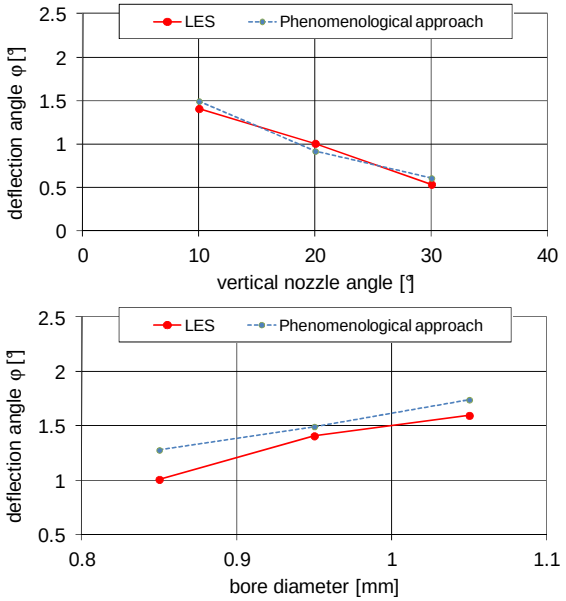

Fig. 11: Deflection angles of the dense spray core tip; Comparison between LES simulation and phenomenological approach

In Fig. 11 the deflection angles of the dense spray core tip are shown for different nozzle angles and diameters. With increasing redirection of the flow and with increasing bore diameter, the deflection increases. With 0° the quick core breakup, the high fluctuations and the large surface waves make it almost impossible to identify reasonable values. Due to these large uncertainties and as the vertical angles are usually larger than 10°, this case was ignored for the generation of the primary breakup model. The core deflection is calculated by the following equation:

$$\varphi_{core} = 3.4 \cdot \left(\frac{d}{l}\right) \cdot \tan\left(\frac{d}{2 \cdot L_{core}}\right)$$

In Fig. 12 the maximum droplet diameters are shown for the simulated cases. As expected, the diameters increase with the bore diameter and with a less disturbed flow. The maximum droplet diameters are calculated by the following equation:

$$d_{droplet,max} = Const \cdot d \cdot \frac{Re}{We} \cdot \left(\frac{d}{l}\right)^{3/2} \cdot \left(\frac{\mu_f}{\mu_g}\right) \cdot \frac{1}{(1-\sin\alpha)^{0.6}} \quad ; \quad 0° \leq \alpha \leq 40°$$

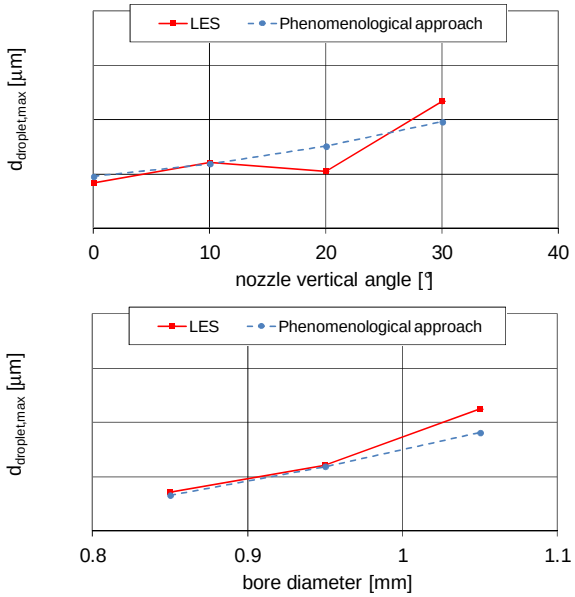

Fig. 12: Max. droplet diameters; Comparison between LES simulation and phenomenological approach

PRIMARY BREAKUP DESCRIPTION

Based on the LES simulations a statistical model was generated to describe the disintegration of the dense spray core into droplets via beta-PDFs.

To analyze the LES results, a layer around the dense core is divided into n segments in nozzle direction and into m segments in circular direction (Fig. 13). For each sector, PDFs for the velocity components, location and droplet diameter were generated based on LES results at several time steps. In each sector, the mass averaged velocities of the fluent phase and the mass centers of the fluent phase are determined for the velocity components and locations respectively. The droplet diameter distribution is computed on basis of the fluent mass within the segments combined with empirical data. This approach will be validated and further developed in the future on the basis of PDA-measurements.

In the next step, correlations were found to generate Presumed PDFs for each parameter – location (x, y, z), velocity (u, v, w) and droplet diameter. Therefore, mean

values and variances are calculated on the basis of thermodynamic conditions, geometric descriptions, deflection of the core and a parameter representing the turbulence level.

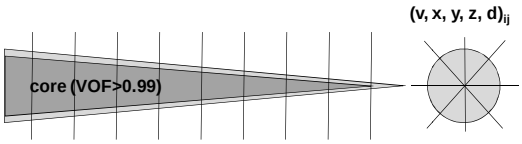

Fig. 13: Layer around the dense core divided into n segments in spray and m segments in circular direction

To calculate absolute values out of these presumed normalized PDFs, either mean or maximum magnitudes are required. The phenomenological approaches presented in the chapter before are used to estimate the breakup length of the dense core, the deflection of the spray and the maximum droplet diameter. The maximum velocity is calculated by Bernoulli equation, whereas the discharge coefficients were derived from the in-nozzle flow simulations.

In a first step the model was compared to data from LES simulations. Therefore Euler-Langrangian spray simulations applying the PDFs, core lengths etc. for the droplet initialization derived from LES simulations were compared to simulations using the Presumed PDFs. Exemplarily, for 10° nozzle angle the evaporated fuel concentration is compared in cross-sections in Fig. 14 (top). The temporal location of the gravity centre of the evaporated fuel is shown for both cases at the bottom. The first point represents the location after t=0.5 ms, the last point after t=5 ms. In z-direction the prediction of the gravity center is similar for both models. In y-direction a difference between both models has to be stated at the beginning. Afterwards the development and the location of the gravity center also correlates in y-direction. The spray simulation based on the statistical primary breakup modeling well represents the simulation that is based on the primary breakup modeled by LES simulations. However, in the near future, the deviation after start of injection will be analyzed in more detail.

The primary breakup model was also validated against experimental data. Results of Euler-Lagrangian spray simulations were compared to shadow images, obtained in the SCC under different operating conditions. The full process in the SCC was simulated, including the inlet flow to gain realistic initial conditions for the spray simulations.

Fig. 15 shows a comparison of a shadow image and the simulations using the Presumed PDF primary breakup model and a conventional model at p=90 bar, T=900 K and swirl. Using conventional models a sharp edge on the upwind side of the spray is observed. This sharp kink doesn't occur, if the statistical primary breakup model is applied. The spray generated with the new statistical model looks reasonable, compared to the shadowgraph image.

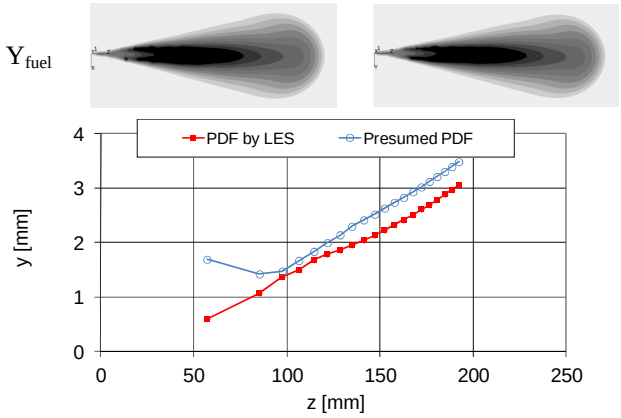

Fig. 14: Evaporated fuel concentration and location of the gravity center of the evaporated fuel ($0.5 \leq t/ms \leq 5$) for different approaches to model the primary breakup; vertical nozzle angle 10°

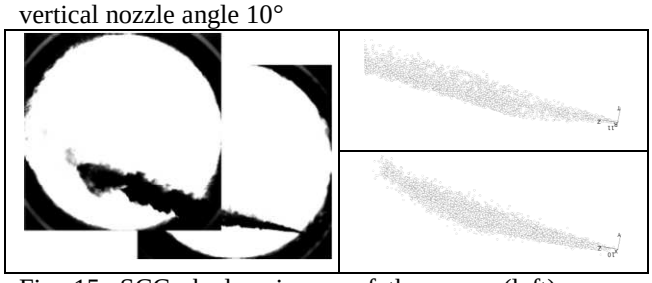

Fig. 15: SCC shadow image of the spray (left); spray modeled conventionally (right, top) and with Presumed PDF approach (right, bottom), p=90 bar / T=900 K, swirl

Fig. 16 shows the corresponding comparison of the spray penetration depth determined experimentally and by CFD simulation depending on time. The spray cone angles are given in Table 3.

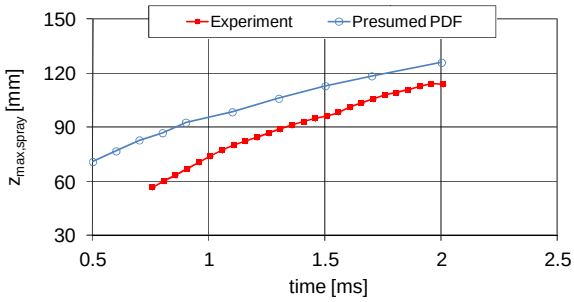

Fig. 16: Comparison of the spray penetration depth determined experimentally and by simulation, p=90 bar / T=900 K, swirl

In general a good agreement between experiment and simulation can be stated so far. However, the penetration depth is still over predicted whereas the cone angles are under predicted (φ_{exp}=18.6°, φ_{sim}=17.2°). The larger difference at start of injection is related to the way how the development of a dense core is modeled after SOI. Currently the formation of the spray core at SOI is calculated as function of mean fuel flow velocity and maximum core length and it is assumed that the dense core develops from SOI on. In reality the sack hole is not to 100% filled up with fuel before the needle opens. The time until sack hole and nozzle are filled up with fuel and until the fuel starts to form a spray is not yet accurately

described. The approach will be reviewed and adapted to experimental data in the next project phase.

Other possible reasons might be found in the analysis and post-processing of the LES simulations. Both, the post-processing of LES simulations as well as the phenomenological approaches require more validation data. Therefore additional SCC investigations including PDA-measurements are scheduled in the near future to determine the droplet diameter distribution. Another reason might be related to the secondary breakup modeling. Due to the changes made in the primary breakup model, the secondary breakup modeling might be reviewed and adapted to the current status.

	Experiment	Simulation
upper	15.7	12.0
lower	-3	-5.0
cone	18.6	17.0

Table 3: Comparison of the spray cone angles determined experimentally and by simulation, p=90 bar / T=900 K, swirl

Furthermore the model was applied to a full engine combustion simulation including sequential injection. Fig. 17 shows for illustration reasons the temperature for conventional models on the left and for the PDF approach on the right in cross sections of the combustion chamber. In general, higher temperature gradients and colder temperatures near the nozzle can be observed. This is due to the modeling of the full cone and the generation of the droplets around the liquid core as well as the higher differentiation of the model.

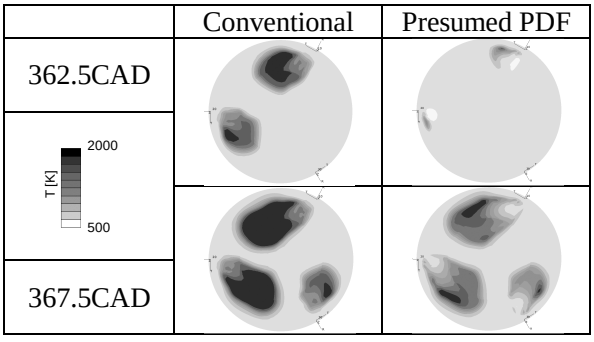

Fig. 17: Temperature in the combustion chamber using conventional models and the PDF approach

CONCLUSIONS

The in-nozzle flow and primary breakup of large marine diesel engines was investigated numerically. It was shown that the spray and droplet formation in large two stroke engines is highly unsymmetrical. Disturbances and a sharp redirection of the flow into the nozzle orifice lead to a deflection of the dense fuel core and eccentricities of the nozzle bore induce a wrinkling up and rotation of the dense core around its central axis.

As existing models do not describe this type of spray breakup, a model to simulate the primary breakup in Euler-Lagrangian spray simulations was generated. This model was validated against LES data and good accordance was stated. Afterwards the SCC as well as first full engine combustion simulations were performed. So far, satisfying results were obtained. However, deviations between simulation and experiment still exist, considering the penetration depth and the spray cone angles. Therefore PDA-measurements will be performed in the near future to generate more data for the validation of the model and the routines to generate PDFs either based on phenomenological approaches or on LES simulations. Furthermore the extension of the model for eccentric nozzles and rotating liquid cores is part of HERCULES C, starting in early 2012.

ACKNOWLEDGEMENTS

A considerable portion of the present work has been conducted as part of HERCULES B within EC contract SCP7-GA-2008-217878 and the authors are grateful for the financial support by the Swiss Federal Government (SBF & BFE). The collaboration with all partners in this project is particularly acknowledged.

NOMENCLATURE

d	Nozzle diameter	x,y,z	Location
$d_{droplet}$	Droplet diameter	z_{max}	Max. core length
f	Fluid (as index)	L_{core}	Dense core length
g	Gas (as index)	α	Vert. nozzle angle
l	Nozzle bore length	φ	Spray cone angle
p	Gas pressure	φ_{core}	Core defl. angle
t	Time	μ	Viscosity
v	Velocity	ρ	Density

REFERENCES

[1] Arcoumanis C., Gavaises M., French B.: “Effect of Fuel Injection Process on the Structure of Diesel Sprays”, SAE 970799

[2] Nishimura A., Assanis D.: “A Model for Primary Diesel Fuel Atomization Based on Cavitation Bubble Collapse Energy”, 8th ICLASS, pp1249-1256

[3] Baumgarten C., Stegemann J., Merker G.:“A New Model for Cavitation Induced Primary Break-up of Diesel Sprays“, ILASS-Europe, 2002

[4] Reitz D., Diwakar R.: “Structure of High-Pressure Fuel Sprays”, SAE 870598

[5] Huh K., Gosman A.: “A Phenomenological Model of Diesel Spray Atomization”, Proc Int Conf on Multiphase Flows, 1991, Tsukuba, Japan

[6] Baumgarten C.: “Mixture Formation in Internal Combustion Engines”, Springer, 2006

[7] Schulz R., et al.: “Assessing the Performance of Spray and Combustion Simulation Tools against Reference Data Obtained in a Spray Combustion Chamber Representative of Large Two-Stroke Diesel Engine Combustion Systems”, CIMAC Congress 2010, Bergen

[8] Herrmann K., et al.: "Validation and Initial Application of a Novel Spray Combustion Chamber Representative of Large Two-Stroke Diesel Engine Combustion Systems", ICLASS 2009

[9] Hiroyasu H., Arai M.: “Structures of Fuel Sprays in Diesel Engines”, SAE 900475